JOURNAL OF KOREA SOCIETY OF PACKAGING
SCIENCE & TECHNOLOGY. Vol. 15, No. 3 99~104 (2009)

# Effect of Clay Type and Concentration on Optical, Tensile and Water Vapor Barrier Properties of Soy Protein Isolate/Clay Nanocomposite Films

**Jong-Whan Rhim†**

*Department of Food Engineering, Mokpo National University, 560 Muanro, Chungkyemyon, Muangun 534-729, Jeonnam, Republic of Korea*

**Abstract** Soy protein isolate (SPI)-based nanocomposite films with three different types of nanoclays, such as Cloisite $Na^+$, Cloisite 20A, and Cloisite 30B, were prepared using a solution casting method, and their optical, tensile, and water vapor barrier properties were determined to investigate the effect of nano-clay type on film properties. Among the tested nanoclays, Cloisite $Na^+$, a hydrophilic montmorillonite (MMT), exhibited the highest transparency with least opaqueness, the highest tensile strength, and the highest water vapor barrier properties, indicating Cloisite $Na^+$ is the most compatible with SPI polymer matrix to form nanocomposite films. The film properties of SPI/Cloisite $Na^+$ nanocomposite films were strongly dependent on the concentration of the clay. Film properties such as optical, tensile, and water vapor barrier properties improved significantly ($p<0.05$) as the concentration of clay increased. However, the effectiveness of addition of the clay reduced above a certain level (*i.e.*, 5wt%), indicating that there is an optimum amount of clay addition to exploit the full advantage of nanocmposite films.

**Keywords** Soy protein isolate, Nanocomposite films, Montmorillonite, Organo-clays, Tensile Properties, Water vapor permeability

## Introduction

Public concerns about the waste disposal problems caused by non-biodegradabilty of petroleum-derived plastics used for packaging of food and non-food materials, depletion of petroleum resources and global warming, the recently experiencing soaring oil price have lead to an interest in biodegradable (sustainable or green) plastic packaging materials[1]. As one of such green polymeric materials, soy protein isolate (SPI) has been widely studied to develop biodegradable/edible films or coatings being used as barriers to solute and gas and tbenhance quality as well as shelf-life of foods[2,3]. Soy protein is an attractive biopolymer, because it is an abundant and annually renewable agro-polymer with good film forming properties[4,5]. Besides the biodegradability of soy protein films, soy protein-based films exhibit effective barrier properties against lipids, gases such as oxygen and carbon dioxide, and aroma compounds[6-8]. However, the SPI-based films indicate main drawbacks such as lower mechanical strength and high water sensitivity compared to commodity plastic films due to its hydrophilic nature. To overcome such problems, several approaches have been performed including modification of polymer network through formation of intra- or intermolecular covalent crosslinkings by treatment with heat[9], addition of chemical cross-linking agents[10], or treatment with enzymes[11]. Another approach was to prepare a blend or bilayer films with hydrophobic biopolymers such as polycaprolactone[12], poly (lactide)[13], or lipids[14].

Benefits of using layered silicate nanoparticles (nanoclays) for improving mechanical, chemical, and water vapor permeability properties of polymers have been recognized recently[15-18]. Such polymers that have reinforced with small amount (less than 5% by weight) of nanoclays are called polymer nanocomposites, which is a good demonstration of nanotechnology. Nanoclays are a class of clay minerals with a phyllosilicate or sheet structure with a platelet thickness of about 1 nm with high aspect ratio (ratio of length to thickness) about 50~1000 and have considerably large surface area, about 750 $m^2/g$[19]. The layered silicate filled polymer composites exhibit extraordinary enhancement of mechanical, gas barrier and other physicochemical properties at low level of filler concentration, compared with pure polymer and conventional microcomposites[20,21]. However, most work done on polymer/clay nano-

†Corresponding Author : Jong-Whan Rhim
Department of Food Engineering, Mokpo National University, 560 Muanro, Chungkyemyon, Muangun 534-729, Jeonnam, Republic of Korea
E-mail : <jwrhim@mokpo.ac.kr>

composites has focused mainly on synthetic polymers[15-18]. Nevertheless, only a limited number of works has been reported on the biopolymer-based nanocomposites[22-25].

The main objectives of this study were to prepare SPI-based nanocomposite films and to determine the effects of different types of nanoclays and their concentration on the film properties, such as optical, tensile and water vapor barrier properties.

## Materials and Methods

### 1. Materials

Soy protein isolate (minimum 90% protein on dry weight basis, Supro 620, SPI) was obtained from Protein Technologies International (St. Louis, MO, USA), and glycerol was purchased from Duksan Pure Chemicals Co., Ltd. (Ansan, Korea). Three types of montmorillonite (MMT) nanoclays including one unmodified MMT (Cloisite $Na^+$) and two organically modified MMTs (Cloisite 20A and Cloisite 30B) were obtained from Southern Clay Co. (Gonzales, TX, USA). The organic modifiers of the Cloisite 20A and 30B are dimethyl dehydrogenated tallow quaternary ammonium and methyl tallow bis-2-hydroxyethyl quaternary ammonium, respectively[26].

### 2. Preparation of films

SPI film solutions were prepared by slowly dissolving 5 g of SPI in a constantly stirring mixture of distilled water (100 mL) and glycerol (2.5 g). The solution pH was adjusted to 10 ± 0.1 with 1 N sodium hydroxide solution and then was heated for 20 min at 70°C in a constant-temperature water bath. For preparation of the nanocomposite film solutions (5% w/w clay relative to SPI), SPI solution and clay suspension were prepared separately. First, SPI solution was prepared by dissolving 5 g of SPI in 50 mL of distilled water and heating as before. Three different types of clay (Cloisite $Na^+$, Cloisite 30B, and Cloisite 20A) were used to test the effect of clay type. Clay suspensions were prepared by mixing 0.25 g of nanoclay in 50 mL of distilled water by using a magnetic stirrer for 1 hr, followed by sonication for 30 min by using a bath type ultrasonicator (Ultra Cleaner FS140H, Fisher Scientific, Pittsburg, PA, USA) at 60°C after adding 2.5 g of glycerol. Then the protein solutions were mixed slowly with the clay suspension and the pH of the mixture was adjusted by using the previously mentioned method, and sonicated again with the use of a probe sonicator (VCX-750, Sonics & Materials, Inc., Newtown, CT, USA) for 30 min. Among the tested nano-clays, Cloisite 20A, which is the most hydrophobic, required more vigorous mixing and further sonication to obtain an adequate degree of dispersion. In addition, SPI/Cloisite $Na^+$ nanocomposite films were prepared with varying clay concentration, *i.e.*, 0, 1, 2.5, 5, 7.5, and 10% (w/w, based on SPI), to test the effect of clay content. The film-forming solutions were poured onto a leveled Teflon (Cole-Parmer Instrument Co., Chicago, IL, USA)-coated glass plate (24 × 30cm) framed on four sides which were spread evenly with a bent glass rod, and were allowed to dry for about 24 hr at room temperature (≈23°C). The resulting films were peeled from the plates.

### 3. X-ray Diffraction (XRD) analysis

Structures of pristine nanoclays and nanoclays in the film matrix were evaluated by XRD measurements. A PANalytical Xpert pro MRD diffractometer (40 kV, 30 mA; Amsterdam, Netherland) equipped with Cu Kα radiation with a wavelength of 0.1542 nm at a scanning rate 0.4°/min was used. Samples were scanned over the range of diffraction angle of $2\theta$= 2-10° with a scanning rate of 0.4°/min at room temperature. The interlayer *d*-spacing was determined by using Bragg's diffraction equation:

$$\lambda = 2\ d_{001}\ \sin\ \theta$$

where, $d_{001}$ is interlayer distance of (001) diffraction face, $\theta$ is diffraction position, and $\lambda$ is the wavelength[27].

### 4. Film thickness and conditioning

Film thickness was measured by using a hand-held micrometer (No. 7326, Mitutoyo Manufacturing Co., Ltd., Tokyo, Japan) with the accuracy of 0.01 mm. Five thickness measurements were taken on each testing specimen and the average value was used in tensile strength (TS) and water vapor permeability (WVP) calculations. All film samples were conditioned for at least 48 hr in a constant-temperature humidity chamber (Model FX 1077, Jeiotech Co., Ltd., Seoul, Korea) at the temperature of 25°C and the relative humidity (RH) of 50% before testing.

### 5. Transparency ($T_{660}$) and opacity

Transparency of films were determined by measuring percent transmittance at 660 nm using a spectrophotometer (8452A Diode Array Spectrophotometer, Hewlett Packard, Palo Alto, CA, USA)[27]. Opacity of films was calculated as follows[28]:

$$\text{Opacity} = A_{600}/x$$

where $A_{600}$ is absorbance at 600 nm measured using the same spectrophotometer and x is film thickness in mm.

### 6. Tensile strength (TS) and percentage elongation at break (E)

For the tensile tests, film specimens were cut into rectangular shapes that were 2.54 cm wide and 15 cm long with the use of a precision double-blade cutter (model LB02/A, Metrotec, S.A., San Sebastian, Spain). TS and E of each film

were measured by using a Model 4465 Instron Universal Testing Machine (Instron Engineering Corp., Canton, MA, USA) in accordance with the ASTM-D882 standard method. For the tensile test, initial grip separation and cross-head speed were set at 50 mm and at 500 mm/min, respectively. Value of TS was calculated by dividing the maximum load by initial cross-sectional area of the film, and E was calculated by dividing extension at rupture of the film by initial length of the film (50 mm) multiplied by 100.

### 7. Water vapor permeability (WVP)

Water vapor transmission rate (WVTR) of SPI-based films was determined by using a gravimetric cup method in accordance with the ASTM E96-95 standard method. Then WVP of the film was calculated by using the following equation:

$$WVP = \frac{WVTR \times l}{\Delta p}$$

where, WVTR is steady state water vapor transmission rate, $l$ is the film thickness and $\Delta p$ is the water vapor partial pressure difference across the two sides of the film. The actual $\Delta P$ value between both sides of the film was determined by using the method proposed by Gennadios *et al.*[29].

### 8. Statistical analysis

Measurements of each property were triplicated for TS, E, and WVP with individually prepared films as the replicated experimental units. SPSS for Windows (SPSS Inc., Chicago, IL) was used to test analysis of variance (ANOVA) and then a Duncan's multiple range test was performed to determine the significant difference between treatments at a 95% confidence level.

## Results and Discussion

### 1. XRD analysis

Figure 1 shows XRD patterns of three different nanoclays used for the test. Each clay shows characteristic diffraction peaks at $2\theta = 7.15$, 4.71 and 3.43° for Cloisite $Na^+$, Cloisite 30B and Cloisite 20A, respectively. Basal spacing ($d_{001}$ spacing) of the clays was calculated with the use of the Bragg's equation. They were 1.24, 1.88 and 2.58 nm for Cloisite $Na^+$, Cloisite 30B and Cloisite 20A, respectively. This indicates the interlayer gallery spacing of Cloisite 30B and Cloisite 20A increased by 0.64 and 1.34 nm through modification of natural MMT (Cloisite $Na^+$) by ion-exchange reactions with cationic surfactants such as methyl tallow bis-2-hydroxyethyl quaternary ammonium and dimethyl dehydrogenated tallow quaternary ammonium for Cloisite 30B and Cloisite 20A, respectively. It is interesting to note that there is still a minor diffraction peak at $2\theta = 7.15°$ in Cloisite 20A, which indicates $Na^+$ in the MMT clay has not exchanged completely with the ammonium ions leading to a less regular organization of the layers in the clay structure.

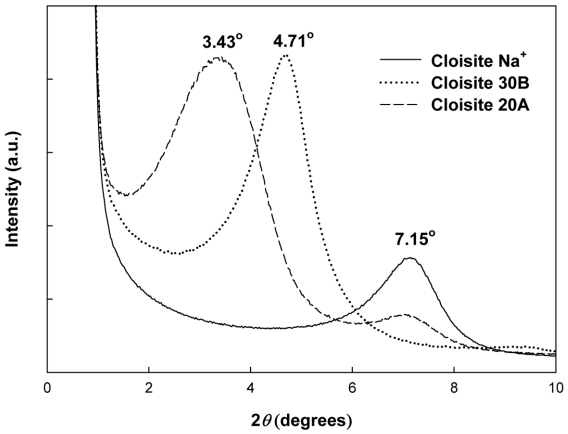


**Fig. 1.** XRD patterns of three different types of pristine nanoclays.

### 2. Effect of clay type

Formation and properties of nanocomposite films are greatly affected by the types of nano-clay depending on their compatibility between polymer matrix and nanoclay[15,16]. Flexible and free-standing SPI and SPI-based nanocomposite films were prepared with three different types of nanoclay, *i.e.*, Cloisite $Na^+$, Cloisite 30B and Cloisite 20A. Cloisite $Na^+$ is an unmodified MMT with pristine layered silicates containing hydrated $Na^+$ ions. Obviously, in this pristine state, the layered silicates are miscible with hydrophilic polymers[23]. On the other hand, Cloisite 30B and Cloisite 20A are organically modified MMTs with quaternary alkylammonium cations to improve the compatibility with non-hydrophilic organic polymers. Due to the properties of ion-exchanged alkylammonium cations, Cloisite 20A is very hydrophobic and it is not easily dispersed in a hydrophilic biopolymer solution, while Cloisite 30B is less hydrophobic and mixes relatively well with biopolymer solution[27].

Table 1 shows the results on the effect of types of nanoclay on film properties. The thickness of SPI films was not changed significantly ($p > 0.05$) with addition of small amount of clay minerals (5% w/w of SPI) in all of nanocomposite films. The control SPI films were transparent and pliable with greenish-yellow tint. Transparency ($T_{660}$) and opacity of SPI films changed greatly after compositing with nano-clays. Transparency of SPI films composited with Cloisite $Na^+$ and Cloisite 30B increased significantly ($p < 0.05$), while that of nanocomposite film with Cloisite 20A decreased. On the contrary, opacity of nanocomposite films increased except for Cloisite $Na^+$ nanocomposite film. As minor disadvantages of nanoclays on polymers, decreased transparency have been

**Table 1.** Effect of type of nanoclays on optical and tensile properties and water vapor permeability of SPI-based nanocomposite films[1)]

| Film | Thickness (μm) | $T_{660}$ (%) | Opacity | TS (MPa) | E (%) | WVP ($\times 10^9$ g.m/m$^2$.s.Pa) |
|---|---|---|---|---|---|---|
| SPI control | 88.4 ± 3.6$^a$ | 56.0 ± 4.6$^b$ | 2.51 ± 0.06$^b$ | 4.80 ± 0.24$^a$ | 172.5 ± 53.1$^b$ | 2.75 ± 0.51$^b$ |
| SPI/Cloisite $Na^+$ | 88.7 ± 5.8$^a$ | 78.6 ± 0.7$^d$ | 1.75 ± 0.00$^a$ | 7.49 ± 0.62$^b$ | 57.7 ± 3.6$^a$ | 1.67 ± 0.46$^a$ |
| SPI/Cloisite 30B | 88.6 ± 2.7$^a$ | 65.3 ± 1.9$^c$ | 2.80 ± 0.04$^b$ | 4.85 ± 0.33$^a$ | 63.8 ± 18.1$^a$ | 2.58 ± 0.35$^b$ |
| SPI/Cloisite 20A | 86.3 ± 5.9$^a$ | 36.5 ± 2.1$^a$ | 5.84 ± 0.03$^c$ | 4.58 ± 0.15$^a$ | 29.4 ± 3.8$^a$ | 2.79 ± 0.16$^b$ |

[1)]Means of three replicates ± standard deviation. Any two means in the same columnfollowed by the same letter are not significantly different ($p > 0.05$) by Duncan's multiple range test. ($T_{660}$ : transparency; TS: tensile strength; E: elongation at break; WVP: water vapor permeability)

reported with various clay/polymer nanocomposite films[27,30)]. Rhim[27)] reported a slight decrease in transparency (*i.e.*, 1-2% depending on clay concentration) of chitosan/Cloisite 30B nanocomposite films. However, in the case of SPI/Cloisite $Na^+$ nanocomposite film, $T_{660}$ increased by 40% and opacity decreased by 30% compared with the control SPI film. It has been reported that materials may present different electronic properties in the nanoscale range, which in turn affects its optical properties and consequently results in increased transparency in well-developed nanocomposite films[16,23)]. This indirectly indicates that Cloisite $Na^+$ is the most compatible with SPI to make a well-developed nanocomposite.

Tensile properties of SPI films were also affected after compositing with nanoclays depending on clay type. TS of nanocomposite films with organically modified nano-clays has not changed significantly ($p > 0.05$). However, that with Cloisite $Na^+$ increased more than 50% compared with the control SPI film. E of all the nanocomposite films decreased by 60~83% compared with the control SPI film. Increase in TS of the SPI/Cloisite $Na^+$ nanocomposite film is mainly attributed to a possible strain-induced alignment of the nanoclay layers in the SPI matrix and strong interaction between them via the formation of hydrogen bonds[15,16)]. The increase in mechanical strength with a sacrifice of flexibility (*i.e.*, decrease in E) has been frequently observed with various nanocomposite films[15,16,22-24)].

Also, WVP of SPI films was changed after compositing with nanoclays. However, the degree of change was strongly dependent on the type of nanoclay. WVP of SPI films composited with Cloisite $Na^+$ decreased significantly ($p < 0.05$) from $2.75 \times 10^{-9}$ g.m/m$^2$.s.Pa to $1.67 \times 10^{-9}$ g.m/m$^2$.s.Pa, while those with Cloisite 30 B and Cloisite 20A did not change significantly. This indicates the hydrophilic nanoclay is more compatible with hydrophilic SPI and consequently it is well mixed and distributed in the SPI polymer matrix compared with less hydrophilic or hydrophobic organoclays. A well mixed and evenly distributed layered silicates are believed to increase the gas barrier properties of nanocomposite films by creating a tortuous path that retards the progress of gas molecule through the polymer matrix[31)].

In general, three possible structures can be formed when nanoclays are mixed with polymers, *i.e.*, immiscible tactoids, intercalated or exfoliated composites[15,16,22-24)]. The immiscible tactoids, frequently observed in conventional microcomposites, result in agglomeration of the clay in the polymer matrix and poor mechanical and barrier properties. The intercalated nanocomposites result from the penetration of polymer chains into the interlayer region of the clay, resulting in an ordered multilayer structure with alternating polymer/clay layers at a repeated distance of a few nanometers. The exfoliated nanocomposites involve extensive polymer penetration, with the clay layers delaminated and randomly dispersed in the polymer matrix, which have been reported to exhibit the best properties due to the optimal interaction between clay and polymer matrix[31)]. Only intercalated or exfoliated structured forms are composed of real nanocomposites with improved film properties[15,22-24)]. The results on the optical, mechanical, and water vapor barrier properties of SPI/clay nanocomposite films indicated that Cloisite $Na^+$ is the most compatible with SPI to make nanocomposite films. Therefore, Cloisite $Na^+$ was used to test the effect of clay content on the film properties.

## 3. Effect of clay content

SPI/Cloisite $Na^+$ nanocomposite films were prepared with the varying amount of the clay and the results on their film properties are shown in Table 2. Though film thickness seems to decrease slightly with increase of clay content, they did not change significantly ($p > 0.05$), which indicates that clay addition in small amount does not affect thickness of the film. Optical properties of SPI and SPI/Cloisite $Na^+$ nanocomposite films determined by transparency ($T_{660}$) and opacity indicates that the transparency and opacity of the nanocomposite films improved significantly ($p < 0.05$), *i.e.*, the nanocomposite films became more transparent and less opaque compared with the SPI control films. The nanocomposite films were the most transparent and least opaque when 1 wt% of clay was mixed with the SPI film matrix and then decreased in transparency and increased in opacity with increase of the clay content. This indicates that the clay has been mixed well with

**Table 2.** Effect of nanoclay concentration on optical and tensile properties and water vapor permeability of SPI/Cloisite $Na^+$ nanocomposite films[1)]

| Clay Conc. (%, w/w) | Thickness (μm) | $T_{660}$ (%) | Opacity | TS (MPa) | E(%) | WVP ($\times 10^9$ g.m/m$^2$.s.Pa) |
|---|---|---|---|---|---|---|
| control | $88.4 \pm 3.6^a$ | $56.0 \pm 4.6^a$ | $2.51 \pm 0.06^c$ | $4.80 \pm 0.24^a$ | $172.5 \pm 53.1^c$ | $2.75 \pm 0.51^d$ |
| 1 | $88.0 \pm 9.8^a$ | $80.6 \pm 1.1^c$ | $0.94 \pm 0.05^a$ | $6.18 \pm 1.40^{ab}$ | $107.6 \pm 46.4^b$ | $2.28 \pm 0.11^{cd}$ |
| 2.5 | $83.4 \pm 11.2^a$ | $80.2 \pm 1.4^c$ | $1.16 \pm 0.04^{ab}$ | $7.61 \pm 1.50^{bc}$ | $70.9 \pm 26.9^{ab}$ | $2.22 \pm 0.26^{cd}$ |
| 5 | $88.7 \pm 5.8^a$ | $78.6 \pm 0.7^{bc}$ | $1.17 \pm 0.00^{ab}$ | $7.49 \pm 0.62^{bc}$ | $57.7 \pm 3.6^{ab}$ | $1.67 \pm 0.46^{ab}$ |
| 7.5 | $86.9 \pm 3.5^a$ | $78.3 \pm 2.8^{bc}$ | $1.57 \pm 0.01^b$ | $9.88 \pm 0.37^d$ | $50.1 \pm 7.8^{ab}$ | $1.77 \pm 0.36^{ab}$ |
| 10 | $82.4 \pm 7.1^a$ | $75.8 \pm 1.9^b$ | $1.66 \pm 0.01^b$ | $12.47 \pm 2.11^e$ | $30.3 \pm 9.0^a$ | $1.57 \pm 0.14^a$ |

[1)]Means of three replicates ± standard deviation. Any two means in the same column followed by the same letter are not significantly different ($p > 0.05$) by Duncan's multiple range test. ($T_{660}$: transparency; TS: tensile strength; E: elongation at break; WVP: water vapor permeability)

the SPI and completely distributed between the polymer matrix at a low clay concentration (*i.e.*, 1 wt%), which is frequently observed with well-developed nanocomposites like exfoliated ones[16,23)]. The XRD pattern of SPI and SPI/1% Cloisite $Na^+$ nanocomposite films (Fig. 2) indicates that the clay has been completely exfoliated in the polymer matrix. Change in the optical properties of the nanocomposite films (*i.e.*, decrease in $T_{660}$ and increase in opacity with increased amount of clay content) may be attributed to the decreased miscibility or less evenly distributed clays in the polymer matrix.

Tensile properties were also greatly influenced by compositing with Cloisite $Na^+$. TS of SPI films increased from 4.80 MPa to 6.18~12.47 MPa, while E decreased from 172.5% to 107.6-30.3% depending on the clay content. Apparently, the film became tougher and less flexible as the clay content increased above 5 wt%. It is generally observed that mechanical strength of nanocomposite film increased with the sacrifice in the flexibility[27,30)].

WVP of SPI films decreased significantly ($p < 0.05$) by compositing with Cloisite $Na^+$. It decreased linearly up to clay content of 5 wt% and then leveled off. Generally, the layered structure of nanoclays in a well-developed nanocomposite films obstructs the transmission of water vapor through the film matrix or delays the diffusing water vapor pathway due to tortuosity[21,32)] resulting in decreased WVP. However, addition of clay into polymer above certain level limits its effectiveness. This is probably because clays added more than saturated content are not evenly distributed in the polymer matrix, or remain as tactoids and do not provide a tortuous pathway for water vapor.

In conclusion, SPI/clay nanocomposite films were prepared with three different types of nanoclays and properties of SPI/clay nanocomposite films such as optical, tensile, and water vapor barrier properties, were greatly influenced by the type of nanoclay and its concentration. Among the tested clays, hydrophilic MMT (Cloisite $Na^+$) exhibited the highest interfacial compatibility with the SPI polymer matrix and the optimum level of the clay addition was found to be less than 5 wt%.

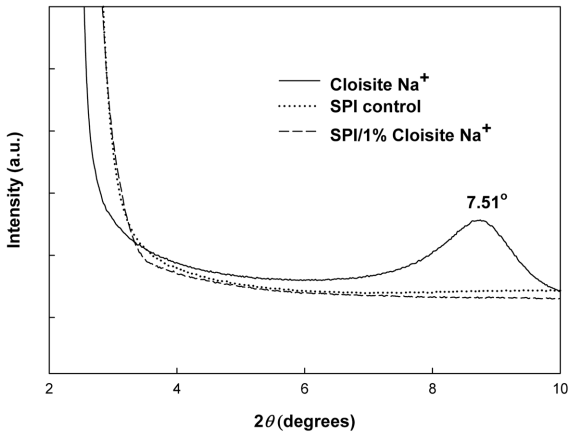


**Fig. 2.** XRD patterns of SPI and SPI/1% Cloisite nanocomposite films.

## Acknowledgments

This work was supported by the Research Grant (2009) of Mokpo National University.

## References

1. Mohanty, A.K., Misra, M., Drzal, L.T., Selke, S.E., Harte, B.R., and Hinrichsen, G. 2005. Natural fibers, biopolymers, and biocomposites: an introduction. pp. 1-36. In: Natural fibers, biopolymers, and biocomposites. Mohanty, A.K., Misra, M., and Drzal, L.T. (eds.), CRC Press, Boca Raton, FL. USA.
2. Gennadios, A., McHugh, T.H., Weller, C.L., and Krochta, J.M. 1994. Edible coatings and films based on proteins. pp. 201-277. In: Edible Coatings and Films to Improve Food Quality. Krochta, J.M., Baldwin, E., and Nisperos-Carriedo, M.O. (eds.) Technomic Publishing Co., Lancaster, PA. USA.
3. Park, S.K., Hettiarachychy, N.S., and Ju, Z.Y., and Genna-

dios, A. 2002. Formation and properties of soy protein films and coatings. pp. 123-137. In: Protein-based Films and Coatings. Gennadios, A. (ed.) CRC Press, Boca Raton, FL. USA.
4. Swain, S.N., Biswal, S.M., Nanda, P.K., and Nayak, P.L. 2004. Biodegradable soy-based plastics: Opportunities and challenges. J. Polym. Environ. 12: 35-42.
5. Zhang, J., Mungara, P., and Jane, J. 2001. Mechanical and thermal properties of extruded soy protein sheets. Polymer 42: 2569-2578.
6. Rhim, J.W., Gennadios, A., Lee, J.J., Weller, C.L., and Hanna, M.A. 2003. Biodegradation of cast soy protein films by *Aspergillus oryzae* and *Bacillus subtilis*. Food Sci. Biotechnol. 12:96-99.
7. Gontard, N. and Guilbert, S. 1994. Biopackaging: Technology and properties of edible and/or biodegradable material of agricultural origin. pp. 159-181. In: Food packaging and preservation. Mathlouthi, M. (ed.) Blackie Academic & professional, London, UK.
8. Krochta, J.M. and De Mulder-Johnston, C. 1997. Edible and biodegradable polymer films: Challenge and opportunities. Food Technol. 40(12): 47-59.
9. Gennadios, A., Ghorpade, V.M., Weller, C.L., and Hanna, M.A. 1996. Heat curing of soy protein films. Trans. ASAE. 39: 575-579.
10. Rhim, J.W. and Weller C.L. 2000. Properties of formaldehyde adsorbed soy protein isolate films. Food Sci. Biotechnol. 9: 228-233.
11. Stuchell, Y.M. and Krochta, J.M. 1994. Enzymatic treatments and thermal effects on edible soy protein films. J. Food Sci. 59: 1332-1337.
12. Mungara, P., Chang, T., Zhu, J., and Jane, J. 2002. processing and properties of plastics made from soy protein polyester blends. J. Polym. Environ. 10: 31-37.
13. Rhim, J.W., Mohanty, A.K., Singh, S.P., and Ng, P.K.W. 2006. Preparation and properties of biodegradable multilayer films based on soy protein isolate and poly(lactide). Ind. Eng. Chem. Res. 45: 3059-3066.
14. Rhim, J.W., Wu, Y., Weller, C.L., and Schnepf, M. 1999. Physical characteristics of emulsified soy protein-fatty acid composite films. Sci. Alimentas 19: 57-71.
15. Alexandre, M. and Dubois, P. 2000. Polymer-layered silicate nanocomposites: preparation, properties and use of a new class of materials. Mater. Sci. Eng. 28: 1-63.
16. Ray, S.S. and Okamoto, M. 2003. Polymer/layered silicate nanocomposites: a review from preparation to processing. Prog. Polym. Sci. 28: 1539-1641.
17. Fedullo, N., Sorlier, E., Sclavons, M., Bailly, C., Lefebvre, J.M., and Devaux, J. 2007. Polymer-based nanocomposites: Overviews, applications and perspectives. Prog. Org. Coatings 58: 87-95.
18. Paul, D.R., and Robeson, L.M. 2008. Polymer nanotechnology: Nanocomposites. Polymer 49: 3187-3204.
19. Sorrentino, A., Gorrasi, G., and Vittoria, V. 2007. Potential perspectives of bio-nanocomposites for food packaging applications. Trends Food Sci. Technol. 18: 84-95.
20. Uyama, H., Kuwabara, M., Tsujimoto, T., Nakano, M., Usuki, A., and Kobayashi S. 2003. Green nanocomposite from renewable resources: Plant oil-clay hybrid materials. Chem. Mater. 15: 2492-2494.
21. Sorrentino, A., Gorrasi, G., Tortora, M., and Vittoria, V. 2006. Barrier properties of polymer/clay nanocomposites. pp. 273-292. In: Polymer nanocomposites Mai, Y.W. and Yu, Z.Z. (eds.), Woodhead Publishing Ltd., Cambridge, UK.
22. Pandey, J.K., Kumarm A.P., Misra, M., Mohanty, A.K., Drzal, L.T., and Singh, R.P. 2005. Recent advances in biodegradable nanocomposites. J. Nanosci. Nanotechnol. 5: 497-526.
23. Ray, S.S. and Bousmina, M. 2005. Biodegradable polymers and their layered silicate nanocomoposites: In greening the 21st century materials world. Prog. Mat. Sci. 50: 962-1079.
24. Rhim, J.W., Ng, P.K.W. 2007. Natural biopolymer-based nanocomposite films for packaging applications. Crit. Rev. Food Sci. Nutr. 47: 411-433.
25. Zhao, R., Torley, P., and Halley, P.J. 2008. Emerging biodegradable materials: starch- and protein-based bio-nanocomposites. J. Mat. Sci. 43: 3058-3071.
26. Hong, S.I. and Rhim, J.W. 2008. Antimicrobial activity of organically modified nano-clays. J. Nanosci. Nanotechnol. 8: 5818-5824.
27. Rhim, J.W. 2006. The effect of clay concentration on mechanical and water barrier properties of chitosan-based nanocomposite films. Food Sci. Biotechnol. 15: 925-930.
28. Giménez, B., Gómez-Estaca, J., Alemán, A., Gómez-Guillén, M.C., and Mentero, M.P. 2009. Physico-chemical and film forming properties of giant squid (*Dosidicus gigas*) gelatin. Food Hydrocolloids 23; 585-592.
29. Gennadios, A., Weller, C.L., and Gooding, C.H. 1994. Measurement errors in water vapor permeability of highly permeable, hydrophilic edible films. J. Food Eng. 21: 395-409.
30. Yu, Y.H., Lin, C.J., Yeh, J.M., and Lin, W.H. 2003. Preparation and properties of poly(vinyl alcohol)-clay nanocomposite materials. Polymer 44: 3553-3560.
31. Adame, D. and Beall, G.W. 2009. Direct measurement of the constrained polymer region in polyamide/clay nanocomposites and the implications for gas diffusion. Appl. Clay Sci. 42: 545-552.
32. Bharadwaj, R.K. 2001. Modeling the barrier properties of polymer-layered silicate nanocomposites. Macromolecules 34: 9189-9192.